Research Article

Journal of PeptideScience

Received: 27 May 2009 Revised: 29 July 2009 Accepted: 4 August 2009 Published online in Wiley Interscience: 28 October 2009

(www.interscience.com) DOI 10.1002/psc.1179

Peptide T exhibits a well-defined structure in fluorinated solvent at low temperature

Tran-Chin Yang,[a] Jennifer Rendell,[a] Wayne Gulliver[b,c] and Valerie Booth[a,d]*

The structure of Peptide T was determined by solution NMR spectroscopy, under strong structure-inducing conditions: 40% hexafluoro-2-propanol aqueous solution at 5 °C. Under these conditions it was possible to detect medium-range NOEs for the first time for this peptide. This allowed a much better-defined structure to be determined for Peptide T in comparison with earlier NMR and computational studies. Peptide structures consistent with the experimental restraints were generated using a restrained MD simulation with a full empirical force field. Residues 4–8 of Peptide T take on a well-defined structure with a heavy atom RMSD of 0.78 Å. The structure is stabilized by hydrogen bonding to side-chain oxygen atoms of Thr 4 and Thr 8, as well as backbone hydrogen bonding between residues 5 and 7 that forms this region into a classic γ-turn.

Keywords: fluorinated solvent; HIV-1; psoriasis

Introduction

Peptide T (ASTTTNYT), termed for its high content of threonine, is derived from the V2 region of glycoprotein gp120 of the HIV [1]. Interest in this peptide has been peaked by its ability to block HIV-1 infection of human T cells [2], its potential capability to resolve psoriatic lesions [3–5], and its ability to attenuate neuroinflammation associated with Alzheimer's disease [6]. The mechanisms of Peptide T are not well understood, but it has been suggested that interactions with the chemokine receptor CCR5 play an important role [7,8].

Given the therapeutic potential of Peptide T, it is not surprising that there have been a number of studies aimed at determining its structure. Such efforts have included computer simulation [9,10] and experimental NMR studies in water [11], aqueous mixtures of DMSO, DMF and ethylene glycol [12]. In these studies, Peptide T displayed, at best, only a very mild preference for any particular configuration. And the studies exhibited no consensus as to what the mild preferences are.

In order to induce a better-defined structure in Peptide T, we took advantage of the strong structure-inducing conditions offered by the combination of low temperature and aqueous fluorinated solvent. The energetically favourable conformation of a peptide under structure-inducing conditions can reveal its receptor-bound conformation [13,14]. Low temperature 'unmasks' receptor binding motifs in small peptides by reducing the effects of entropy [14,15] and fluorinated solvents such as TFE and HFIP are thought to induce structure in part by strengthening local electrostatic interactions such as hydrogen bonds [16,17].

The combination of 40% HFIP aqueous solution and low temperature (5 °C) did have the desired effect of inducing a better-defined conformation in Peptide T than has been observed before. Under these conditions we were able to observe several medium-range NOEs, i.e. correlations that indicate distances closer than 4.5–5 Å between hydrogen nuclei of residues that are not sequential in the primary sequence. These medium-range NOEs, combined with sequential NOEs, were enough to unambiguously establish a single well-defined conformation for Peptide T.

Materials and Methods

NMR

Peptide T, (D-Ala')-peptide T amide acetate, was supplied by Bachem California Inc., CA, USA, and used without further purification. The peptide was dissolved in 40% HFIP, 50% H_2O, 10% D_2O, with 0.2 mM sodium azide and 0.2 mM 2,2-dimethyl-2-silapentane-5-sulfonate (DSS), and the pH adjusted to 5.0. The peptide concentration was 2 mM. All one- (1D) and two-dimensional (2D) NMR spectra were acquired with watergate water suppression on a Bruker Avance 500 MHz spectrometer with a TXI probe (Karlsruhe, Germany). The recycle time for 1D and 2D experiments employed was 1.5, and 2.0 s, respectively. The number of averaging scans for 2D experiments was 48 for NOESY, and 72 for TOCSY and DQF-COSY experiments. NOESY spectra were acquired with a range of mixing time (up to 500 ms) to check for spin diffusion. Spectra were processed using NMRPipe [18], and chemical shift assignment was performed using Sparky Software [19].

NOEs were quantified using peak intensity from the NOESY spectrum with a mixing time of 300 ms. Twenty-six sequential and six medium-range unambiguous NOEs were input into the CNS structure calculation programme as distance restraints [20]. The

* *Correspondence to: Valerie Booth, Department of Biochemistry, Memorial University of Newfoundland, St. John's, NL A1B 3X9, Canada. E-mail: vbooth@mun.ca*

a *Department of Biochemistry, Memorial University of Newfoundland, St. John's, NL, Canada*

b *Division of Dermatology, Memorial University of Newfoundland, St. John's, NL, Canada*

c *NewLab Clinical Research Inc., St. John's, NL, Canada*

d *Department of Physics and Physical Oceanography, Memorial University of Newfoundland, St. John's, NL, Canada*

Journal of PeptideScience

lowest energy structure output from CNS was retained and used as the starting structure for the MD run.

MD Simulation

NVT MD simulation was performed using the Gromacs package [21] with the OPLS-AA all-atom force field [22]. The solvent was TIP4P water [23] with the property FLEXIBLE. The starting structure for the simulation was the NMR structure of Peptide T, calculated by CNS as described above. The system consisted of 45 072 atoms (116 amino acid atoms and 11 239 TIP4P water molecules) in a 70 Å length box with cubic periodic boundary conditions. Energy minimization was performed with the initial peptide structure in vacuum and then again after the solvent was added. At this point the coordinates of all the Peptide T atoms were fixed and 10 ps of MD simulation was performed to equilibrate the system at 310 K. Following this, a 50 ns MD simulation was run. For the first 40 ns of the run, distance restraints were placed on the atom pairs indicated by the NMR NOE data (i.e. the 26 sequential and 6 medium-range NOEs). For the last 10 ns of the simulation, all of the distance restraints were removed. The Berendsen thermostat [24] was used with a 0.1 ps coupling time constant to maintain the temperature at 310 K. The simulation time step was set to 2 fs, the neighbour list generation cutoff was 9 Å and the non-bonded cutoffs were 9 Å for short-range electrostatics and 10 Å for van der Waals interactions.

Analysis of the MD trajectory was done using the analysis routines within Gromacs, as well as the program Molmol [25]. Hydrogen bonds were detected using the default Molmol parameters, distance <2.40 Å, angle $<35.0^{\circ}$.

Results

2D NOESY NMR spectra of Peptide T in 40% HFIP aqueous solution were acquired at several temperatures (data not shown). At higher temperatures there were few inter-residue cross peaks, but at 5 °C a large number of inter-residue cross peaks were observed, indicating that the peptide was relatively structured at low temperatures. Assignment of chemical shifts was accomplished using 2D TOCSY and NOESY data. Chemical shifts could be assigned to all the hydrogen atoms normally observable in NMR spectra, with the exception of the β protons of Thr 8 (Table 1).

The NOESY spectrum indicated 26 sequential NOEs and 6 medium-range NOEs (Figure 1; Table 2). The medium-range NOEs, i.e. correlations that indicate close spatial distances between atoms from residues that are not sequential, were of particular note since they indicate a relatively well-defined compact structure. In order to ensure that these NOESY cross peaks were not influenced by spin diffusion, a series of 2D NOESY with varying mixing times were acquired (data not shown), the analysis of which indicated no sign of spin diffusion at 300 ms, the mixing time used to generate the distance restraints input into the structure calculations and MD simulation. The medium-range NOEs observed were between residues 5 and 7, as well as 4 and 6, indicating a relatively well-defined, compact structure of the peptide from residues 4 to 7.

The NOEs were used to define distance restraints that were input into CNS [20], one of the standard software packages for generating three-dimensional protein structures from NMR data. However, since CNS is optimized for use with larger proteins with more dense distant restraint data, it is not well suited for use with small peptides and their relatively sparse distance restraints. Therefore, restrained MD simulations with a full empirical force field were used to better characterize the conformational space consistent with the experimental data, as well as to provide insight into the interactions that stabilize the peptide in the observed conformation. The CNS-generated-structure was used as the starting structure for a Gromacs [21] MD simulation. For the first 40 ns of the simulation, the system was restrained using the distances derived from the sequential and medium-range NOEs, and for the last 10 ns these restraints were removed. The resulting

Table 1. NMR chemical shifts of Peptide T in 40% HFIP aqueous solution at 5 °C

Residue	Position	1H (ppm)
Ala 1	α	4.246
	β	1.641
Ser 2	N	8.896
	α	4.641
	$\beta 1$	4.047
	$\beta 2$	3.970
Thr 3	N	8.516
	α	4.560
	β	4.418
	$\gamma 2$	1.326
Thr 4	N	8.341
	α	4.495
	β	4.359
	$\gamma 2$	1.301
Thr 5	N	8.207
	α	4.377
	β	4.236
	$\gamma 2$	1.200
Asn 6	N	8.469
	α	4.801
	$\beta 1$	2.859
	$\beta 2$	2.787
	$\delta 1$	7.642
	$\delta 2$	6.913
Tyr 7	N	8.283
	α	4.664
	$\beta 1$	3.154
	$\beta 2$	3.088
	δ	7.217
	ε	6.921
Thr 8	N	8.023
	α	4.335
	$\gamma 2$	1.244

Table 2. Medium-range NOEs observed for Peptide T in 40% HFIP aqueous solvent

Thr 4 Hγ2 to Asn 6 HN
Thr 5 Hγ2 to Tyr 7 HD
Thr 5 Hγ2 to Tyr 7 HE
Thr 5 Hγ2 to Tyr 7 HN
Thr 5 HB to Tyr 7 HN
Thr 5 HA to Tyr 7 HN

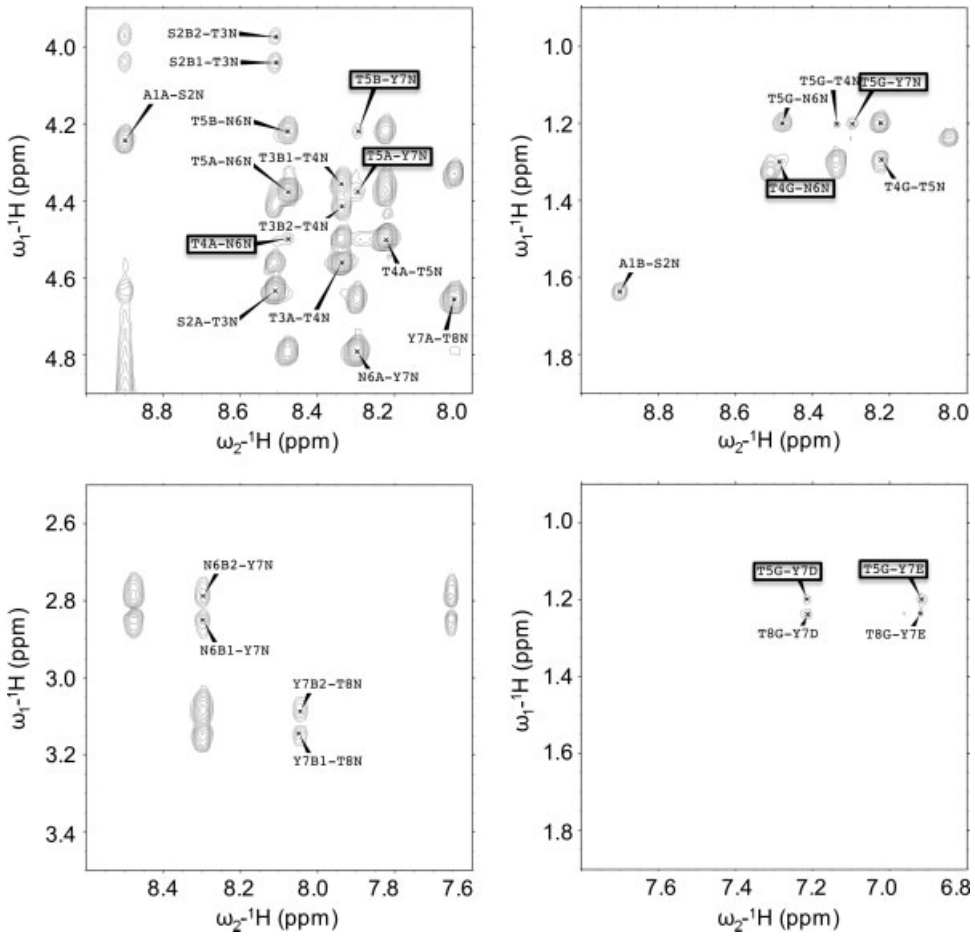

Figure 1. Selected sections of the 300 ms mixing time NOESY spectrum of Peptide T in 40% HFIP aqueous solution at 5 °C. Selected NOEs are labelled, with the medium-range NOEs indicated by boxes around the label. The figure was prepared using Sparky [19].

MD structures were similar to the CNS-generated structures (e.g. heavy atom RMSD for residues 4–8 of the representative CNS and MD-generated structures was 1.8 Å) and like the CNS structures were consistent with the experimental data. However, since unlike with CNS, the MD structures were generated using a full empirical forcefield, the MD structures were able to reveal the favourable interactions, such as hydrogen bonds, likely to be stabilizing the experimental structure.

A variety of parameters were examined as a function of simulation time to indicate the time period at which the simulation could be considered to be equilibrated. These parameters included all the individual energy components and the pseudo energy associated with the distance restraints, as well as peptide RMSD, backbone dihedral angles and hydrogen bonding patterns. All of these parameters appeared to have stabilized within the first 20 ns of simulation and therefore the 20–40 ns range of the simulation was used for the analysis of Peptide T's conformation. In this time range, Peptide T exhibited a well-defined structure (Figure 2(A) and (B)) from residue 4 to 8 with a heavy atom RMSD of 0.78 Å. Most of the backbone dihedral angles for residues in this region are also quite well-defined (Table 3).

Upon removal of the NOE-derived distance restraints at 40 ns, there was very little change in the structure of the peptide (Figure 2(B)), even after 10 ns of simulation without restraints. This indicates that the distance restraints did not unnaturally overconstrain the conformation of the peptide. It should also be noted that while the NMR data were acquired in 40% HFIP, the simulations were done in pure water. That the conformation of the peptide defined by the distance restraints measured in HFIP was still stable in the absence of HFIP suggests that the observed structure is not an artifact of the specific solvent employed in the NMR studies and that this conformation is likely to be sampled by the peptide even in the absence of HFIP.

Table 3. Average backbone dihedral angles and standard deviations for residues in the structured region of Peptide T, taken from the 20–40 ns range of the restrained MD simulation

Residue	ϕ (°)	ψ (°)
Thr 4	-137.9 ± 29.2	-141.9 ± 68.8
Thr 5	-83.6 ± 23.3	-32.3 ± 21.1
Asn 6	86.3 ± 9.8	-28.4 ± 26.7
Tyr 7	-109.9 ± 37.8	-53.8 ± 77.6
Thr 8	-105.8 ± 29.3	26.1 ± 57.0

Figure 2(A) shows a representative structure of Peptide T along with the medium-range NOEs shown in green. The NOEs define a compact structure centred around residues 5–7. Examination of the MD trajectory indicates that this configuration is likely stabilized mainly by three hydrogen bonds. Two of these, Thr 5 HN to Thr 4 OG1 and Thr 5 HG1 to Thr 8 OG1, involve

Journal of PeptideScience

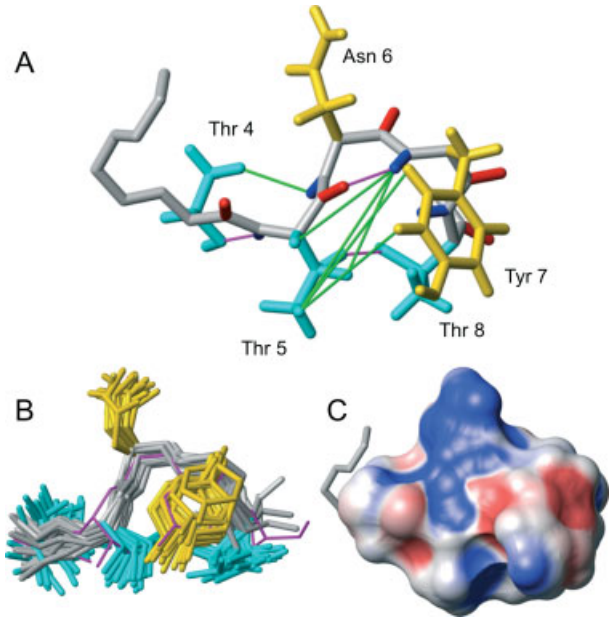

Figure 2. Structure of Peptide T. (A) Representative structure of Peptide T showing the medium-range NOEs in green and the three most prevalent hydrogen bonds in magenta. The entire backbone is shown, but for clarity side-chains 1–3 are ommitted. The backbone is indicated in grey, threonine side-chains in magenta and other side-chains in gold. (B) Ensemble showing snapshots of the peptide every 1 ns during the 20–40 ns portion of the simulation. The structures were aligned using all the backbone and heavy sidechain atoms for residues 4–8 and these are the segments of the peptide that are shown. The structure shown in magenta is the structure 10 ns after the NMR distance restraints were removed from the simulation. (C) Electrostatic surface for residues 4–8 of Peptide T, shown in the same orienation as panel A. All panels were prepared using Molmol [25].

the side-chains of Thr residues. These two hydrogen bonds were present 60% of the time in the 20–40 ns range of the trajectory, and continued to be present after the distance restraints were removed from the simulation. The third major hydrogen bond is between backbone atoms, Tyr 7 HN and Thr 5 O, was observed to be present for 59% of the 20–40 ns portion of the trajectory, and was also retained after the distance restraints were removed. This backbone hydrogen bond matches the pattern for a γ-turn [26]. Examination of the dihedral angles (Table 3) indicates a good match for a classic γ-turn which is defined by ϕ and ψ angles of the central residue within 40° of the standard angles, $\phi = 75°$, $\psi = -64°$. Additional hydrogen bonds were also detected but were observed for smaller portions of the trajectory, such as Thr 8 HG1 to Thr 5 OG1 and Thr 8 HN to 5 Thr OG1, present 22 and 15% of the time, respectively.

An electrostatic surface was calculated for residues 4–8 and is displayed in Figure 2(C). The molecular shape and charge distribution pattern are complex and thus consistent with an ability of the peptide to bind protein receptor target(s) specifically and competitively with the natural receptor ligands.

Discussion

For such a diminutive peptide, Peptide T seems to have received a disproportionately large number of efforts at structure determination [9–12]. The structure determination endeavours have presumably been inspired by Peptide T's potential as a therapeutic molecule for a number of disorders including HIV infection and psoriasis [2,5]. The structural studies performed on Peptide T thus far have revealed only mild structural preferences, as illustrated by the absence of reports of medium or long range NOEs in the NMR spectra, and that these mild preferences depend on the solvent system in which the peptide is placed, for example with Peptide T taking on a γ-turn conformation in aqueous mixtures of ethylene glycol and a type-IV β-turn conformation in aqueous mixtures of DMSO [12].

While there is currently much interest in intrinsically disordered proteins that are able to bind more than one target [27] these proteins probably possess somewhat different folding characteristics from peptides that are unstructured in the absence of their cognate receptor by virtue of their small size [28] rather than the need to bind several targets. There are several examples of such peptides which display predisposed structural preferences in the absence of receptor [15,29–31] although discussions as to if they bind receptors via selection of the correct conformer or folding upon binding are ongoing [32]. Peptide T has been proposed to act by binding to CD4 [33] and/or CCR5 [34,35]. We have attempted to use solution NMR to assess the CD4/Peptide T interaction, however were unable to detect any binding (data not shown). CCR5 is a G-protein coupled receptor, and thus presents major difficulties in terms of obtaining a suitable sample for structural studies. Thus, we are left with the problem of determining the 'active', receptor-bound structure of Peptide T in the absence of receptor.

The receptor-bound conformation of a peptide is determined by enthalpic contacts – both between the peptide and the receptor and within the peptide itself – which overcome the unfavourable change in entropy when the peptide takes on a defined structure upon binding [14]. In many cases it is possible to overcome the entropy barriers to the peptide forming a defined structure in the absence of receptor by lowering the temperature and thus reducing the unfavourable entropic contribution to the Gibb's free energy function, $\otimes G = \otimes H - T \otimes S$. This has the effect of 'revealing' energetically favourable conformations of the peptide. While the conformational energy of the peptide contributes only part of the overall energy of the receptor-peptide complex, it seems unlikely that the peptide would take on an energetically unfavourable conformation in the receptor-bound complex. Thus the energetically favourable conformation revealed at low temperature potentially has the power to reveal the peptide's functional conformation. This has been shown to be the case, for example with the Hox peptide, for which the low temperature conformation and target protein-bound conformation of the peptide have both been determined and appear to coincide [13], as well as chemokine-based peptides whose low temperature structures match each other as well as the structure of a drug targeting the same GPCR [14].

Fluorinated alcohols, such as HFIP, provide an additional means to induce peptide structure [36,37]. Aqueous mixtures comprised of TFE and HFIP are some of the most effective solvents to stabilize protein structure, with HFIP having a much stronger effect than TFE [38–41]. The effects of alcohol on protein structure have been shown to arise from the low polarity of the solvent, which leads to the strengthening of local electrostatic interactions, such as hydrogen bonds. It should be noted though, that fluorinated alcohols are more effective at inducing structure than would be expected based solely on their polarity, and the underlying reasons for this are still unclear. In this work we use the strong structure-inducing conditions provided by the combination of HFIP and low

temperature to induce a well-defined structure in Peptide T. While it is not possible to say for certain that this conformation is similar to the active, receptor-bound conformation, it is hard to imagine why the peptide would take on an energetically unfavourable conformation upon binding the receptor and thus there is good reason to suppose that the structure determined is functionally relevant.

In 40% HFIP aqueous solvent at 5 °C, Peptide T takes on a well-defined structure over residues 4–8, as supported by experimental NMR data consisting of 26 sequential NOEs, and 6 medium-range NOEs, mainly between residues 5 and 7. To our knowledge, this is the first time medium-range NOEs have been reported for this peptide, indicating the peptide takes on a better-defined structure under these conditions than has been observed before. The structure formed by Peptide T centres around a classic γ-turn, stabilized by a hydrogen bond between 7 Tyr HN and 5 Thr O. This type of structure has been observed before in NMR studies of Peptide T in ethylene glycol aqueous solution [12], although in the 2007 study fewer sequential NOEs and no medium-range NOEs were observed, indicating there was less structuring under these conditions. In HFIP aqueous solution at 5 °C, the structuring consists of more than just the γ-turn, with a compact structure defined for the backbone and side-chain atoms of residues 4–8. The MD simulation indicates that in addition to the backbone hydrogen bonding, the observed structure is stabilized by hydrogen bonds involving the side-chains of the threonines at positions 4, 5 and 8.

It should be noted that in different solvent systems, Peptide T has been shown to exhibit other structures, such as type-IV β-turn conformation in aqueous mixtures of DMSO [12]. Thus, while the current study stands apart from earlier ones in having found conditions where this peptide takes on a more defined structure, as indicated by the presence of medium-range NOEs as well as greater numbers of sequential NOEs, and that a more defined structure presumably correlates with a deeper energy minimum in Peptide T's conformational space, it is of course possible that the conformation found in this study is only one of several functionally relevant structures of Peptide T.

Acknowledgement

We acknowledge a CIHR grant given to Valerie Booth (ROP-78967), and Peptide T sample was provided by Advanced ImmuniT. Inc.

References

1 Pert CB, Ruff MR. Peptide t[4-8]: A pentapeptide sequence in the aids virus envelope which blocks infectivity is essentially conserved across nine isolates. *Clin. neuropharmacol.* 1986; **9**(Suppl 4): 482–484.
2 Polianova MT, Ruscetti FW, Pert CB, Tractenberg RE, Leoung G, Strang S, Ruff MR. Antiviral and immunological benefits in hiv patients receiving intranasal peptide t (dapta). *Peptides* 2003; **24**: 1093–1098.
3 Marcusson JA, Lazega D, Pert CB, Ruff MR, Sundquist KG, Wetterberg L. Peptide t and psoriasis. *Acta Derm. Venereol. Suppl.* 1989; **146**: 117–121.
4 Liapi C, Takahashi N, Raynaud F, Evain-Brion D, Anderson WB. Effects of [d-ala1] peptide t-nh2 and hiv envelope glycoprotein gp120 on cyclic amp dependent protein kinases in normal and psoriatic human fibroblasts. *J. Invest. Dermatol.* 1998; **110**: 332–337.
5 Raychaudhuri SK, Raychaudhuri SP, Farber EM. Anti-chemotactic activities of peptide-t: A possible mechanism of actions for its therapeutic effects on psoriasis. *Int. J. Immunopharmacol.* 1998; **20**: 661–667.
6 Rosi S, Pert CB, Ruff MR, McGann-Gramling K, Wenk GL. Chemokine receptor 5 antagonist d-ala-peptide t-amide reduces microglia and astrocyte activation within the hippocampus in a neuroinflammatory rat model of alzheimer's disease. *Neuroscience* 2005; **134**: 671–676.
7 Ruff MR, Polianova M, Yang QE, Leoung GS, Ruscetti FW, Pert CB. Update on d-ala-peptide t-amide (dapta): A viral entry inhibitor that blocks ccr5 chemokine receptors. *Curr. HIV Res.* 2003; **1**: 51–67.
8 Redwine LS, Pert CB, Rone JD, Nixon R, Vance M, Sandler B, Lumpkin MD, Dieter DJ, Ruff MR. Peptide t blocks gp120/ccr5 chemokine receptor-mediated chemotaxis. *Clin. Immunol.* 1999; **93**: 124–131.
9 Centeno NB, Perez JJ. A proposed bioactive conformation of peptide t. *J. Comput. Aided Mol. Des.* 1998; **12**: 7–14.
10 Filizola M, Centeno NB, Perez JJ. Computational study of the conformational domains of peptide t. *J. Pept. Sci.* 1997; **3**: 85–92.
11 De Dios AC, Sears DN, Tycko R. Nmr studies of peptide t, an inhibitor of hiv infectivity, in an aqueous environment. *J. Pept. Sci.* 2004; **10**: 622–630.
12 D'ursi A, Caliendo G, Perissutti E, Santagada V, Severino B, Albrizio S, Bifulco G, Spisani S, Temussi PA. Conformation-activity relationship of peptide t and new pseudocyclic hexapeptide analogs. *J. Pept. Sci.* 2007; **13**: 413–421.
13 Slupsky CM, Sykes DB, Gay GL, Sykes BD. The hoxb1 hexapeptide is a prefolded domain: Implications for the pbx1/hox interaction. *Protein Sci.* 2001; **10**: 1244–1253.
14 Booth VK, Slupsky CM, Clark-Lewis I, Sykes BD. Unmasking ligand binding motifs: Identification of a chemokine receptor motif by nmr studies of antagonist peptides. *J. Mol. Biol.* 2003; **327**: 329–334.
15 Slupsky CM, Spyracopoulos L, Booth VK, Sykes BD, Crump MP. Probing nascent structures in peptides using natural abundance 13c nmr relaxation and reduced spectral density mapping. *Proteins* 2007; **67**: 18–30.
16 Hong DP, Hoshino M, Kuboi R, Goto Y. Clustering of fluorine-substituted alcohols as a factor responsible for their marked effects on proteins and peptides. *JACS* 1999; **121**: 8427–8433.
17 Hirota N, Mizuno K, Goto Y. Cooperative alpha-helix formation of beta-lactoglobulin and melittin induced by hexafluoroisopropanol. *Protein Sci.* 1997; **6**: 416–421.
18 Delaglio F, Grzesiek S, Vuister GW, Zhu G, Pfeifer J, Bax A. Nmrpipe: A multidimensional spectral processing system based on unix pipes. *J. Biomol. NMR* 1995; **6**: 277–293.
19 Goddard TD, Kneller DG. *Sparky 3*, University of California, San Francisco, CA.
20 Brunger AT, Adams PD, Clore GM, DeLano WL, Gros P, Grosse-Kunstleve RW, Jiang JS, Kuszewski J, Nilges M, Pannu NS, Read RJ, Rice LM, Simonson T, Warren GL. Crystallography & nmr system: A new software suite for macromolecular structure determination. *Acta Crystallogr. D Biol. Crystallogr.* 1998; **54**: 905–921.
21 Lindahl E, Hess B, van der Spoel D. Gromacs 3.0: A package for molecular simulation and trajectory analysis. *J. Mol. Model.* 2001; **7**: 306–317.
22 Kaminski GA, Friesner RA, Tirado-Rives J, Jorgensen WL. Evaluation and reparametrization of the opls-aa force field for proteins via comparison with accurate quantum chemical calculations on peptides. *J. Phys. Chem. B* 2001; **105**: 6474–6487.
23 Jorgensen WL, Chandrasekhar J, Madura JD, Impey RW, Klein ML. Comparison of simple potential functions for simulating liquid water. *J. Chem. Phys.* 1983; **79**: 926–935.
24 Berendsen HJC, Postma JPM, van Gunsteren WF, Dinola A, Haak JR. Molecular dynamics with coupling to an external bath. *J. Chem. Phys.* 1984; **81**: 3684.
25 Koradi R, Billeter M, Wuthrich K. Molmol: A program for display and analysis of macromolecular structures. *J. Mol. Graph.* 1996; **14**: 51–55, 29–32.
26 Hutchinson EG, Thornton JM. Promotif–a program to identify and analyze structural motifs in proteins. *Protein Sci.* 1996; **5**: 212–220.
27 Tompa P, Szasz C, Buday L. Structural disorder throws new light on moonlighting. *Trends Biochem. Sci.* 2005; **30**: 484–489.
28 Williamson MP, Waltho JP. Peptide structure from nmr. *Chem. Soc. Rev.* 1992; **21**: 227–236.
29 Langelaan DN, Bebbington EM, Reddy T, Rainey JK. Structural insight into g-protein coupled receptor binding by apelin. *Biochemistry* 2009; **48**: 537–548.
30 Yao S, Zhang MM, Yoshikami D, Azam L, Olivera BM, Bulaj G, Norton RS. Structure, dynamics, and selectivity of the sodium

Journal of PeptideScience

channel blocker mu-conotoxin siiia. *Biochemistry* 2008; **47**: 10940–10949.
31 Baryshnikova OK, Rainey JK, Sykes BD. Nuclear magnetic resonance studies of cxc chemokine receptor 4 allosteric peptide agonists in solution. *J. Pept. Res.* 2005; **66**(Suppl 1): 12–21.
32 Wright PE, Dyson HJ. Linking folding and binding. *Curr. Opin. Struct. Biol.* 2009; **19**: 31–38.
33 Ruff MR, Martin BM, Ginns EI, Farrar WL, Pert CB. Cd4 receptor binding peptides that block hiv infectivity cause human monocyte chemotaxis. Relationship to vasoactive intestinal polypeptide. *FEBS Lett.* 1987; **211**: 17–22.
34 Ruff MR, Melendez-Guerrero LM, Yang QE, Ho WZ, Mikovits JW, Pert CB, Ruscetti FA. Peptide t inhibits hiv-1 infection mediated by the chemokine receptor-5 (ccr5). *Antiviral Res.* 2001; **52**: 63–75.
35 Cairns JS, D'Souza MP. Chemokines and hiv-1 second receptors: The therapeutic connection. *Nat. Med.* 1998; **4**: 563–568.
36 Roccatano D, Fioroni M, Zacharias M, Colombo G. Effect of hexafluoroisopropanol alcohol on the structure of melittin: A molecular dynamics simulation study. *Protein Sci.* 2005; **14**: 2582–2589.
37 Fioroni M, Burger K, Mark AE, Roccatano D. Model of 1, 1, 1, 3, 3, 3-hexafluoro-propan-2-ol for molecular dynamics simulations. *J. Phys. Chem. B Condens. Phase* 2001; **105**: 10967–10975.
38 Diaz MD, Fioroni M, Burger K, Berger S. Evidence of complete hydrophobic coating of bombesin by trifluoroethanol in aqueous solution: An nmr spectroscopic and molecular dynamics study. *Chemistry* 2002; **8**: 1663–1669.
39 Fioroni M, Diaz MD, Burger K, Berger S. Solvation phenomena of a tetrapeptide in water/trifluoroethanol and water/ethanol mixtures: A diffusion nmr, intermolecular noe, and molecular dynamics study. *J. Am. Chem. Soc.* 2002; **124**: 7737–7744.
40 Yoshida K, Yamaguchi T, Adachi T, Otomo T, Matsuo D, Takamuku T, Nishi N. Structure and dynamics of hexafluoroisopropanol-water mixtures by x-ray diffraction, small-angle neutron scattering, nmr spectroscopy, and mass spectrometry. *J. Chem. Phys.* 2003; **119**: 6132.
41 Naseem F, Khan RH. Fluoroalcohol-induced stabilization of the alpha-helical intermediates of lentil lectin: Implication for non-hierarchical lectin folding. *Arch. Biochem. Biophys.* 2004; **431**: 215–223.

